Bone 121 (2019) 80–88

Contents lists available at ScienceDirect

Bone

journal homepage: www.elsevier.com/locate/bone

Full Length Article

Weekly teriparatide treatment increases vertebral body strength by improving cortical shell architecture in ovariectomized cynomolgus monkeys☆

Ryuji Fujihara[a], Tasuku Mashiba[a,*], Shingo Yoshitake[a], Satoshi Komatsubara[a], Ken Iwata[a], Ryoko Takao-Kawabata[b], Tetsuji Yamamoto[a]

[a] Department of Orthopedic Surgery, Faculty of Medicine, Kagawa University, 1750-1 Ikenobe, Miki-cho, Kita-gun, Kagawa 761-0793, Japan
[b] Pharmaceutical Research Center, Asahi Kasei Pharma Corporation, 632-1 Mifuku, Izunokuni, Shizuoka 410-2321, Japan

ARTICLE INFO

Keywords:
Teriparatide
Cynomolgus monkey
Vertebral cortical bone
Bone histomorphometry
Bone mechanical property

ABSTRACT

Weekly teriparatide treatment is reported to reduce the incidence of osteoporotic vertebral fractures. However, the effect of weekly teriparatide on cortical bone has not been clarified. This study aimed to examine the effects of weekly teriparatide treatment on bone mass, intracortical structure, and remodeling of the lumbar vertebral cortical shell and its relation to mechanical properties in ovariectomized cynomolgus monkeys. Female monkeys, aged 9 to 15 years, were divided into four groups: (1) SHAM group, (2) ovariectomized group (OVX group), (3) OVX with 1.2 μg/kg once-weekly teriparatide group (LOW group), (4) OVX with 6.0 μg/kg once-weekly teriparatide group (HIGH group). After 18 months, all animals were double-labeled with calcein, and lumbar vertebrae were analyzed with histomorphometry and compressive mechanical tests. Following ovariectomy, we found reductions in the anterior cortical shell area of the vertebrae and reductions in nearly all of the tested vertebral mechanical properties. Weekly teriparatide significantly preserved the anterior cortical shell area and the energy absorption capacity of the lumbar vertebrae in a dose-dependent manner. Multiple regression analyses indicated that improved mechanical properties were more associated with the increased anterior cortical shell area rather than the cancellous bone volume. The intracortical structure of the Haversian canals was also preserved following teriparatide treatment after ovariectomy. These findings suggest the importance of the cortical shell as a therapeutic target in the treatment of osteoporosis. Weekly teriparatide treatment increases the compressive mechanical strength of the lumbar vertebrae by thickening the anterior cortical shell.

1. Introduction

Teriparatide is an anabolic agent used to treated patients with osteoporosis who have an especially high risk of fracture [1]. The anabolic effect of teriparatide on cancellous bone has been demonstrated using iliac crest biopsies from postmenopausal women [2,3] and in animal experiments following ovariectomy [4–8]. Several studies have also revealed the anabolic effect of teriparatide on the cortical bone of the appendicular skeleton, such as on the humerus [9] and femur [10] in ovariectomized (OVX) monkeys, and on the iliac crest [3], femur [11,12], and radius [13] in postmenopausal women. However, few studies have evaluated the effect of teriparatide on the vertebral cortical shell, which serves an important role in vertebral mechanical strength [14,15]. Chen et al. previously reported that the daily administration of teriparatide for 18 months increased the thickness of the cortical shell of lumbar vertebrae and this increase was associated with an increased vertebral compressive strength in ovariectomized cynomolgus monkeys [16]. In their study, however, bone turnover was not examined and the vertebral cortical shell was evaluated only in a single plane.

Although patients are routinely treated with daily teriparatide injections, a weekly treatment regime for teriparatide is already used in Japan [17] and South Korea to treat patients with osteoporosis who have a high fracture risk. Weekly teriparatide treatment was reported to reduce the incidence of osteoporotic vertebral fractures by 78% in postmenopausal women with prevalent vertebral fracture [17]. In ovariectomized cynomolgus monkeys, Saito et al. reported that weekly

☆ Declaration of interest
This work was funded by Asahi Kasei Pharma Corporation and R Takao-Kawabata is an employee of Asahi Kasei Pharma Corporation.

* Correspondence author.
E-mail address: task@med.kagawa-u.ac.jp (T. Mashiba).

https://doi.org/10.1016/j.bone.2019.01.006
Received 15 October 2018; Received in revised form 21 December 2018; Accepted 7 January 2019
Available online 08 January 2019

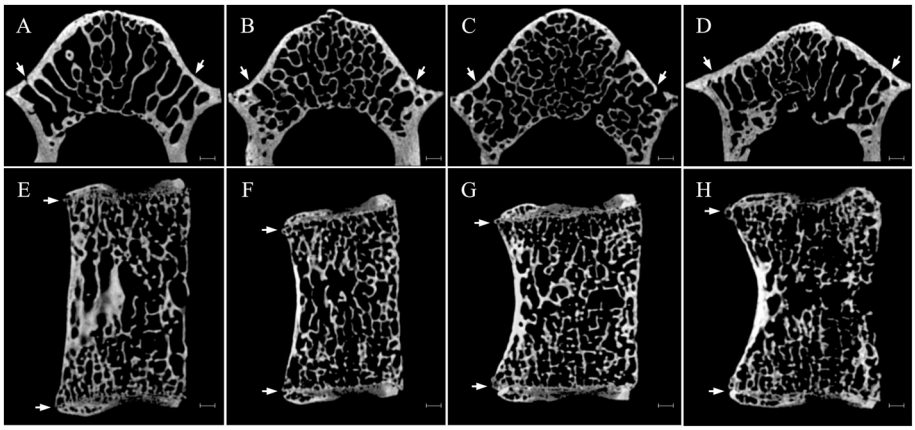

Fig. 1. Representative μCT images of the mid-axial section obtained from L3 (A–D) and the mid-sagittal section obtained from L7 (E–H). The median bone mineral density (BMD) is shown for SHAM (A, E), OVX (B, F), LOW (C, G), and HIGH (D, H) groups. Arrows indicate the boundary of the measured area of the anterior cortical shell. Scale bars, 1 mm.

teriparatide for 18 months increased cancellous bone mass and lumbar vertebral strength [18]; however, the effect of weekly teriparatide treatment on the vertebral cortical shell was not assessed.

The purpose of this study was to investigate the anabolic effects of weekly teriparatide treatment on vertebral cortical bone using multiplanar micro-CT reconstruction, and to determine how this relates to the mechanical properties of the vertebral cortical bone in ovariectomized cynomolgus monkeys. Furthermore, we evaluated the changes in the intracortical structure and remodeling of the cortical shell of the lumbar vertebrae.

2. Methods

2.1. Animals and experimental design

Skeletally mature, female cynomolgus monkeys (aged, 12.0 ± 1.5 years) were purchased from C.V. Universal Fauna (Jakarta Timur, Indonesia), and were acclimated for 6 weeks before the study. Monkeys were kept under controlled conditions at 26 °C ± 2 °C with a 12-h light-dark cycle, and given free access to water and a daily diet of commercial food (approximately 108 g) containing 1.4% calcium and 0.6% phosphorus (Harlan Sprague Dawley Inc., Indianapolis, USA).

Monkeys (body weight, 2.06 to 3.48 kg), without evidence of abnormalities during the acclimation period, were selected and divided into four groups (n = 19 to 20) based on body weight, spine bone mineral density (BMD), and age: (1) SHAM group, (2) OVX group, (3) OVX with low-dose teriparatide (1.2 μg/kg once-weekly) group (LOW group), (4) OVX with high-dose teriparatide (6.0 μg/kg once-weekly) group (HIGH group), as described by Saito et al. [18] Ovariectomy was performed on monkeys in the three treatment groups one week before treatment was commenced; a sham operation was performed for monkeys in the SHAM group. Monkeys in the LOW and HIGH groups were subcutaneously injected once-weekly with teriparatide acetate (Asahi Kasei Pharma Corp., Tokyo, Japan) at 1.2 μg/kg (estimated clinical dose) and 6.0 μg/kg body weight, respectively, for 18 months. Monkeys in the SHAM and OVX groups were subcutaneously injected once-weekly with 0.1% saline containing bovine serum albumin as a vehicle. For bone histomorphometry, all monkeys were double-labeled with intravenous calcein (4 mg/kg; Dojindo Laboratories, Kumamoto, Japan) on days 21 and 7 before sacrifice.

All experimental protocols were approved by the experimental animal ethics committee of Asahi Kasei Pharma Co., and were conducted in accordance with guidelines concerning the management and handling of experimental animals.

2.2. Measurement of bone mineral density

BMD of the lumbar vertebrae (L3 to L5) was measured once before teriparatide treatment and then at 6, 9, 12, and 18 months after treatment using dual-energy X-ray absorptiometry (DPX-α, Lunar Co.). For scanning, monkeys were placed in the supine position and anesthetized with an intramuscular injection of 10 mg/kg of ketamine (Sigma Chemical Co.).

2.3. Bone preparation

Following necropsy, lumbar vertebrae (L3, L4, L7) were harvested. L3 and L4 were wrapped in saline-soaked gauze and kept at −20 °C prior to testing. L7 was fixed with 70% ethanol and embedded in methyl methacrylate-based plastic.

2.4. Measurement of micro-CT

Raw L3 and embedded L7 vertebrae were separately scanned using two types of cone-beam X-ray micro-CT (L3: MCT-CB100MF, Hitachi Medico Technology, Kashima, Japan; L7: ScanXmate-RB090SS150, Comscantecno, Kanagawa, Japan) with the following settings: tube voltage, 55 kV and 70 kV; tube current, 0.1 mA and 0.1 mA; and an isotropic voxel size of 32 μm and 34 μm, respectively.

We measured cancellous bone in the center of the L3 vertebra, approximately 4.5-mm in height on axial sections, and manually delineated the trabecular region approximately 0.2 mm away from endocortical surface. We measured cancellous bone in the L7 vertebra with a 1-mm thickness centered on the mid-sagittal section of the vertebral body and delineated the rectangular shape as the area of interest, 2 mm away from the endplates and 1 mm away from the endocortical surface. Three-dimensional images were constructed and used to determine cancellous bone volume (BV/TV, %) and trabecular thickness (Tb.Th, μm) semi-automatically using TRI/3D-BON software (RATOC System Engineering Corp., Tokyo, Japan) according to the guidelines for the assessment of bone microstructure using micro-CT [19].

Cortical structural parameters were measured on mid-axial images of L3 and mid-sagittal images of L7 (Fig. 1) vertebrae using ImageJ software (National Institutes of Health, USA) [20]. The tissue area (T.Ar) of the mid-axial section of L3 was determined as the area ventral to the transverse process, and the anterior shell cortical area (Ct.Ar) was measured from within the T.Ar. The T.Ar of the mid-sagittal section obtained from L7 was determined as the whole vertebral body, and anterior shell Ct.Ar was measured between the cranial and caudal plates. Cortical thickness (Ct.Th) was directly measured within the anterior cortical shell area on both axial and sagittal sections. The boundary between the cortex and the cancellous bone was determined manually with reference to a previous report that analyzed the cortical bone boundary in the femoral neck [21]. In brief, pores close to the endocortical surface were recognized as cortical bone if their shortest diameters were shorter or equal to the distance from the pores to the endocortical surface. The anterior shell Ct.Ar fraction (Ct.Ar/T.Ar, %) was obtained by dividing the Ct.Ar by the T.Ar.

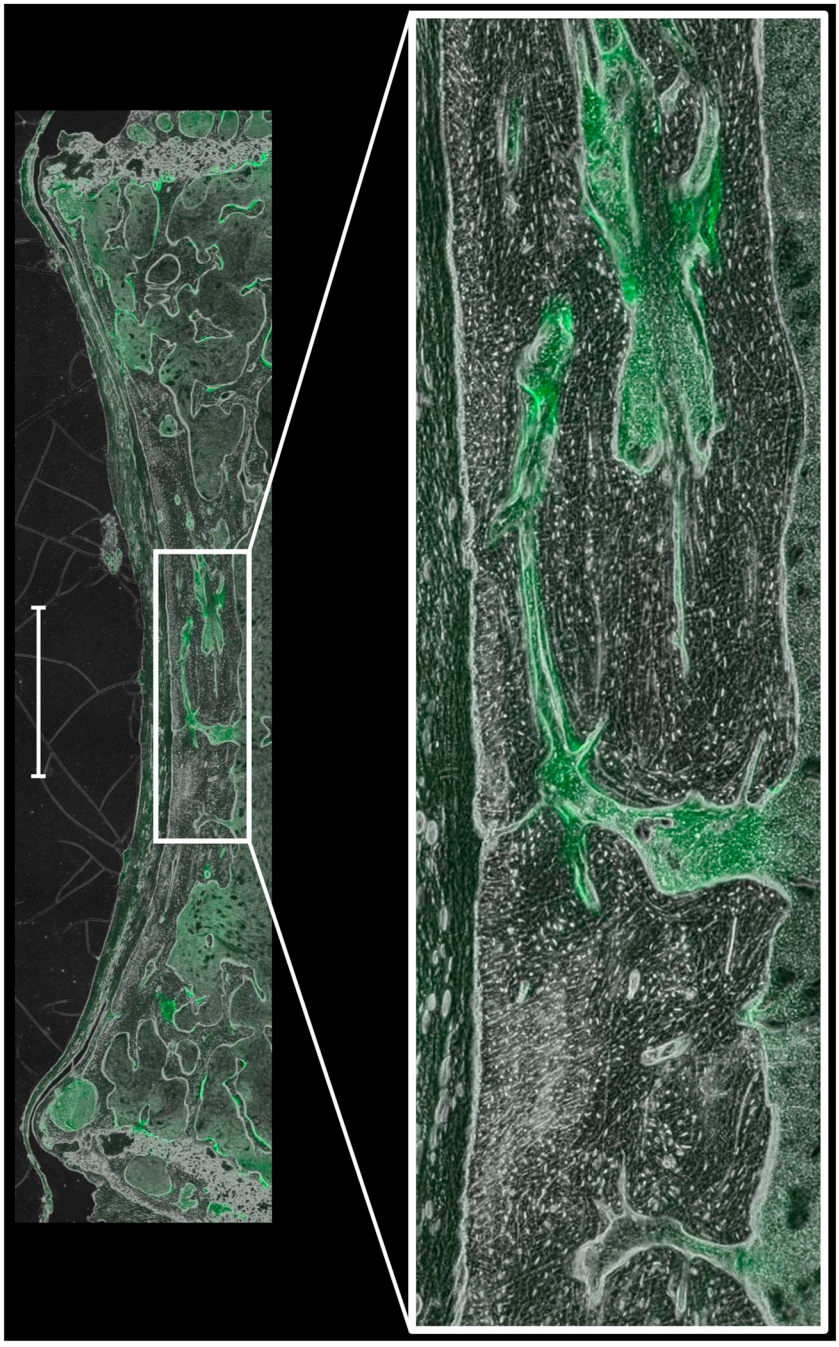

Fig. 2. Anterior cortical shell in a sagittal section of the L7 vertebra obtained using fluorescence phase-contrast imaging. The Haversian canal resembles trabecular bone structure in the anterior cortical shell. Scale bar, 2 mm.

2.5. Cortical bone histomorphometry

Cortical bone remodeling and the structure of the Haversian canals were evaluated using sagittal sections of the L7 vertebra. Although conventional intracortical histomorphometric measurements are usually carried out on transverse sections, they provide limited structural information regarding cortical porosity, and require a specific technique to evaluate intracortical remodeling. Because we sought to evaluate the complicated structure of Haversian canals, we required sagittal sections of the lumbar vertebrae. Haversian canals have a similar structure to that of trabecular bone in the anterior cortical shell, and calcein labeling was occasionally observed along the surface of the Haversian canal under fluorescent light (Fig. 2). Therefore, we used conventional histomorphometric measurements of trabecular bone to evaluate Haversian canal structure and intracortical remodeling.

Resin-embedded L7 vertebrae were sectioned around the mid-sagittal portion with a diamond saw and ground to approximately 30-μm thickness. Digital images of the anterior shell between the growth plates of each vertebra were obtained using a fluorescence phase-contrast microscope (FSX100, Olympus, Tokyo, Japan) at 4.2× magnification, and manual measurements were performed using graphic software (WinROOF2015, Mitani Corporation). One section of the L7 vertebra was measured for each animal.

Mineralized surface (MS/BS, %) was determined as the total of the double-labeled surface plus half the single-labeled surface. Mineral apposition rate (MAR, μm/day) was measured as the mean distance between two consecutive labels divided by the labelling interval. Bone formation rate (BFR/BS, $\mu m^3/\mu m^2$/day) was calculated as the product of MS/BS and MAR. These dynamic parameters were obtained at the

periosteal (Ps), endocortical (Ec), and Haversian (H) surfaces.

Cortical porosity (H.Ar/Ct.Ar, %) was obtained by dividing the Haversian area by the cortical area. Structural parameters of the Haversian canals were calculated using the Haversian area and perimeter, according to the plate model [22–24] and based on standard calculations for Tb.Th, Tb.N, and Tb.Sp, as follows: Haversian thickness (H.Th = 2/(H.Pm/H.Ar), μm), Haversian number (H.N = (H.Ar/Ct.Ar)/H.Th, #/μm), and Haversian separation (H.Sp = (1/H.N) − H.Th, μm). Nomenclature and symbols used are in accordance with the report of the Histomorphometry Nomenclature Committee of American Society for Bone and Mineral Research [25].

2.6. Compression mechanical test

For each L4 vertebra, the posterior pedicle arch, spinous process, and cranial and caudal ends were removed using an Exakt saw (EXAKT, Oklahoma City, OK, USA) to obtain a vertebral body specimen with two parallel surfaces and a height of approximately 7 mm, measured with an electronic caliper. The cross-sectional area was measured from the mid-axial image of the vertebral body using peripheral quantitative CT (XCT-RM, Norland Corp., Fort Atkinson, WI, USA). Compression testing was performed with the specimens placed between two platens in an Instron Mechanical Testing Machine (Instron 4465 retrofitted to 5500), and a load was applied at a displacement rate of 6 mm/min until failure. The load and displacement curve were recorded by Testing Machine Software (Merlin II, Instron). The maximum load at failure (N), stiffness (N/mm), and energy absorption (mJ) were selected manually from the load and displacement curve and then calculated using machine software (Merlin II, Instron). From these parameters, we calculated the intrinsic properties, including ultimate stress (N/mm^2), elastic modulus (MPa), and toughness (MJ/m^3).

2.7. Finite element analysis

Finite element analysis was used to analyze the role of the cortical shell and cancellous bone separately for energy absorption; the mean energy absorption for each group is reported. Image processing for finite element analysis was performed by RATOC System Engineering Corp. (Tokyo, Japan). The finite element model was generated by voxel mesh from μCT data (voxel size of 32 μm) obtained from L3 vertebrae using TRI/3D-FEM-FCS64 software (RATOC System Engineering Corp., Tokyo, Japan). Cortical bone was separated from cancellous bone based on a minimum threshold of 2400 Hounsfield units, and the Young's modulus for each element was calculated based on the cubic BMD function, as described in previous reports [26,27]. In brief, we used Young's modulus value of 3.5 GPa for a BMD of 600 mg/cm^3 and 21.7 GPa for a BMD of 1100 mg/cm^3, where Young's modulus (GPa) was equal to 16.53 $(BMD)^3$. We incorporated a Poisson's ratio of 0.3 for both elements. After conducting a mesh convergence study, a voxel size of 32 μm was used for the finite element analysis. To simulate the compression mechanical test in this study, an axial displacement of 0.02 mm was applied vertically to the cranial portion of the vertebral model with a height of 4.48 mm by using a setting where the caudal portion was restrained.

We analyzed the distribution of von Mises stresses in the cortical and cancellous bones [28]. In a previous fracture analysis, the distribution of the minimum principal strain was shown to simulate the fracture location [29]. Therefore, to quantify the fracture analysis, a minimum principal strain of > 0.5% was defined as the strain that induces fracture, and the fracture load was determined as the level that induces fractures in 2.8% of all voxels.

2.8. Statistical analysis

Statistical analysis was performed using SPSS v22 (IBM Corp., Armonk, NY, USA). Differences among the groups were analyzed by one-way ANOVA. If a significant difference was found, the differences between the groups were analyzed using a Fisher protected least significant difference test. Pearson product-moment correlation coefficient and linear regression analysis were used to assess the relationship between structural and biomechanical parameters using all specimens from all groups. Multiple regression analysis was performed to identify the determinant factors for bone strength. The difference was considered to be significant when $P < 0.05$.

3. Results

3.1. General conditions

There were no significant differences in body weight among monkeys in the treatment groups (data not shown).

3.2. Bone mineral density

We determined the mean (± SD) change in BMD measured before and at 18 months after teriparatide treatment: SHAM, 2.2 ± 4.3%; OVX, −5.7 ± 7.8%; LOW, 4.0 ± 10.7%; HIGH, 4.2 ± 5.5%. The percent changes were significantly lower in the OVX group than in the SHAM group ($P = 0.002$), whereas those in the LOW and HIGH groups were significantly higher than that in the OVX group ($P = 0.0001$, $P = 0.00009$, respectively). Significant BMD increases were also observed at 9 months and 12 months after teriparatide administration (Fig. 3).

3.3. Structural parameters from micro-CT

The ovariectomy procedure had no significant effect on cancellous bone mass in either the axial section of the L3 vertebra or the sagittal section of the L7 vertebra. In contrast, the anterior shell Ct.Ar and Ct.Th were significantly decreased by ovariectomy in both the axial and sagittal sections.

Weekly teriparatide treatment for 18 months increased BV/TV in the L3 axial section compared with the OVX group, but no dose-dependent effect was found between the LOW and HIGH groups (Table 1). There were also no significant changes in BV/TV or Tb.Th for the L7 sagittal section following teriparatide treatment, when compared with the OVX group.

Teriparatide treatment significantly increased the anterior shell Ct.Ar in the L7 sagittal section in a dose-dependent fashion. There was also a tendency for a dose-dependent increase following teriparatide treatment in the L3 axial section, but this did not reach statistical significance. Ct.Th was also increased following high-dose teriparatide treatment as compared with that in the OVX group.

3.4. Histomorphometry of anterior shell

In the OVX group, there were no significant changes in any dynamic bone formation parameters for either the cortical surfaces or the intracortical Haversian surface compared with the SHAM group (Table 2). After 18 months of weekly high-dose teriparatide treatment, only Haversian MAR was increased as compared with that in the OVX group.

There were some significant changes in Haversian structure: H·N was decreased by OVX, and preserved dose-dependently with teriparatide treatment. Although no significant changes were observed in H.Th, the H.Ar/Ct.Ar was reduced by OVX, and tended to be preserved by teriparatide treatment.

3.5. Mechanical properties

The mechanical properties of the vertebrae deteriorated after OVX and were preserved by teriparatide treatment. All parameters except for the elastic modulus were lower in the OVX group than in the SHAM

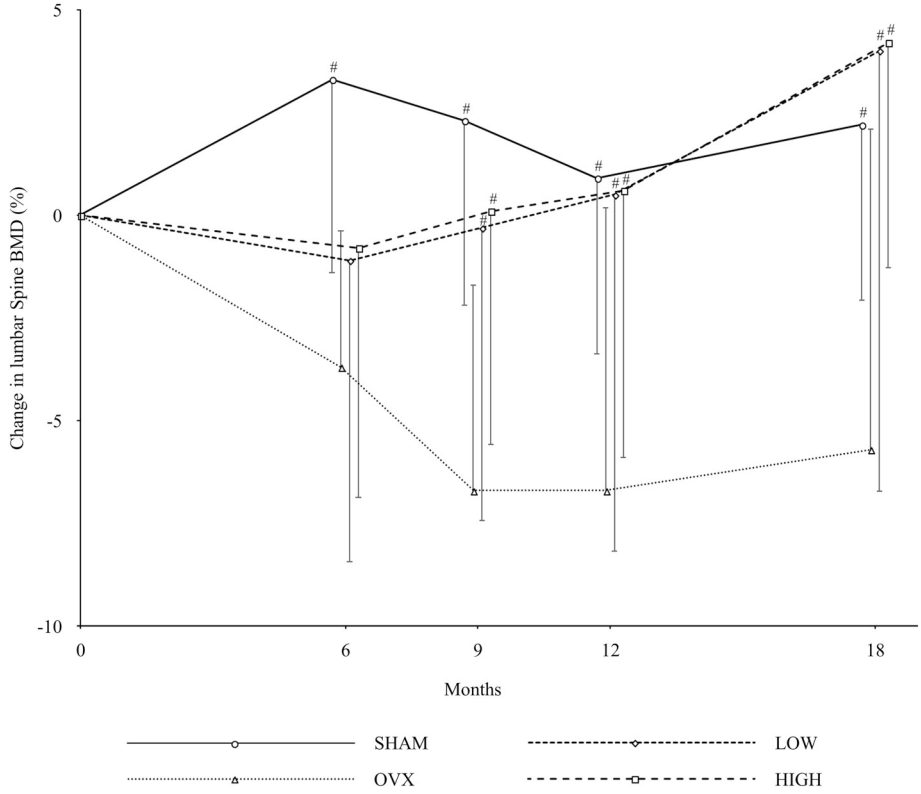

Fig. 3. Percent changes from baseline in lumbar vertebral bone mineral density (BMD). Values are mean percentage change (%) and bars indicate standard deviation. $^{\#}P < 0.05$ versus OVX.

group (Table 3). Energy absorption and toughness were significantly higher in the HIGH group than in the OVX group ($P = 0.009$ and $P = 0.02$, respectively).

3.6. Correlation between structural and mechanical parameters

All parameters pertaining to the vertebral mechanical properties were significantly correlated with the anterior shell Ct.Ar fraction and cancellous bone volume (Fig. 4, Table 4). However, cortical porosity (H.Ar/Ct.Ar) was not correlated with any of the mechanical parameters.

Multiple regression analysis was performed to evaluate which factor determined toughness using Ct.Ar/T.Ar and BV/TV obtained from each L3 axial and L7 sagittal section. We found that toughness was related to both parameters (Table 5). The anterior shell Ct.Ar fraction was more associated with toughness rather than cancellous BV in each L3 axial or L7 sagittal section.

3.7. Finite element analysis for stress and fracture distribution

The distribution of von Mises stresses showed that the cortical shell received larger stress in axial loading than the cancellous bone in all groups (Fig. 5A–D). The minimum principal strain, simulating fracture distribution in the anterior cortical shell, was increased by OVX and decreased by teriparatide treatment (Fig. 5E–L). The quantified fracture load at the cortical shell was approximately 10% higher in the HIGH group than in the OVX group; the fracture loads at the cortical bone were 926, 817, 823, and 915 N in the SHAM, OVX, LOW, and HIGH groups, respectively. By contrast, the fracture load at the cancellous bone was approximately 10% lower in the HIGH group than in the OVX group; the fracture loads at the cancellous bone were 712, 656, 689, and 588 N in the SHAM, OVX, LOW, and HIGH groups, respectively. The fracture loads at the cortical bone simulate the energy absorption values obtained from the compression mechanical test in a representative sample (620, 473, 501, and 669 mJ in the SHAM, OVX, LOW, and HIGH groups, respectively).

Table 1
Structural parameters from μCT.

	SHAM ($n = 19$)	OVX (n = 19)	LOW (n = 19)	HIGH ($n = 20$)
L3 (axial section)				
BV/TV (%)	30.9 ± 3.19	30.4 ± 3.73	34.1 ± 5.43*,#	33.4 ± 4.40#
Tb.Th (μm)	175.8 ± 17.9	165.1 ± 13.4	181.0 ± 19.4#	180.8 ± 23.9#
Ct.Ar/T.Ar (%)	17.5 ± 4.30	13.7 ± 3.48*	14.2 ± 2.46*	16.1 ± 6.69
Ct.Th (μm)	438.3 ± 79.6	315.0 ± 68.0*	354.1 ± 64.2*	439.8 ± 112.6#
L7 (sagittal section)				
BV/TV (%)	33.8 ± 4.30	30.4 ± 5.89	31.8 ± 5.72	28.5 ± 7.02*
Tb.Th (μm)	167.1 ± 22.8	154.5 ± 16.3	170.1 ± 21.7	164.6 ± 28.6
Ct.Ar/T.Ar (%)	3.91 ± 1.15	2.55 ± 0.89*	2.62 ± 0.72*	3.39 ± 1.59#
Ct.Th (μm)	534.7 ± 147.6	368.8 ± 107.1*	357.4 ± 99.3*	475.7 ± 179.0#

Values are expressed as mean ± SD.
* $P < 0.05$ vs. SHAM.
# $P < 0.05$ vs. OVX.

Table 2
Cortical histomorphometry in the anterior shell of L7 vertebrae.

	SHAM (n = 19)	OVX (n = 19)	LOW (n = 19)	HIGH (n = 20)
Dynamic parameters				
Periosteal (Ps)				
Ps.MAR (μm/d)	0.31 ± 0.66	0.11 ± 0.35	0.11 ± 0.34	0.17 ± 0.43
Ps.MS/BS (%)	3.4 ± 4.1	5.6 ± 7.5	4.5 ± 4.8	8.1 ± 11.3
Ps.BFR/BS ($\mu m^3/\mu m^2$/d)	0.033 ± 0.083	0.029 ± 0.10	0.006 ± 0.019	0.046 ± 0.12
Endocortical (Ec)				
Ec.MAR (μm/d)	0.56 ± 0.61	0.74 ± 0.63	0.88 ± 0.55	0.84 ± 0.56
Ec.MS/BS (%)	7.0 ± 4.6	9.1 ± 4.9	8.5 ± 4.5	11.8 ± 11.7*
Ec.BFR/BS ($\mu m^3/\mu m^2$/d)	0.047 ± 0.054	0.092 ± 0.089	0.088 ± 0.074	0.12 ± 0.15*
Haversian (H)				
H.MAR (μm/d)	0.61 ± 0.59	0.38 ± 0.68	0.59 ± 0.58	0.85 ± 0.58#
H.MS/BS (%)	11.8 ± 7.3	13.7 ± 8.2	13.8 ± 9.6	15.8 ± 11.5
H.BFR/BS ($\mu m^3/\mu m^2$/d)	0.086 ± 0.097	0.086 ± 0.17	0.11 ± 0.14	0.16 ± 0.15
Structural parameters				
H·Th (μm)	43.3 ± 15.3	35.9 ± 15.5	39.4 ± 13.1	40.0 ± 15.6
H·N (/mm)	1.0 ± 0.24	0.85 ± 0.31*	0.96 ± 0.25	1.0 ± 0.35#
H.Sp (μm)	958.1 ± 243.2	1352.0 ± 710.8*	1040.7 ± 295.8	1069.8 ± 524.9
H·Ar/Ct.Ar (%)	4.76 ± 2.57	3.16 ± 1.83*	3.82 ± 1.77	4.37 ± 2.63

Values are expressed as mean ± SD.
Numbers of animals with double labels in SHAM, OVX, LOW, and HIGH groups were 4, 2, 2, and 3, respectively, at the periosteal surface, 10, 13, 15, and 16, respectively, at the endocortical surface, and 12, 6, 10, 15, respectively, at the Haversian surface.
* $P < 0.05$ vs. SHAM.
# $P < 0.05$ vs. OVX.

4. Discussion

We investigated the effect of weekly teriparatide treatment for 18 months on cortical bone mass and structure, and on the mechanical properties of lumbar vertebral bodies in ovariectomized cynomolgus monkeys. The results show that bone mass of the anterior cortical shell and mechanical strength of lumbar vertebral body were significantly increased following weekly teriparatide treatment in a dose-dependent fashion. Although the cancellous bone volume was also increased following teriparatide treatment, the increased mechanical properties were more associated with the increase in bone mass of the anterior cortical shell rather than that of the cancellous bone. Furthermore, teriparatide treatment also preserved the intracortical canal structure, as reflected by the change in H·N, probably due to increased intracortical remodeling (Table 2).

In previous studies with large experimental animals with Haversian remodeling systems, the anabolic effect of teriparatide treatment on cortical bone was mainly measured in the appendicular skeleton [9,10,30]. However, to the best of our knowledge, few studies using ovariectomized cynomolgus monkeys have shown the anabolic effects of teriparatide on the vertebral cortical bone. In the study reported by Chen et al. [16], in which ovariectomized monkeys were treated with a daily injection of 1.0 or 5.0 μg/kg teriparatide for 18 months, the cortical bone volume in the lumbar vertebra was dose-dependently increased and had the strongest correlation with compressive vertebral strength. This is consistent with our finding that the increased amount of cortical bone in the anterior shell of the lumbar vertebra was well correlated with vertebral strength parameters (Table 4). Furthermore, finite element analysis revealed that teriparatide treatment decreased the minimum principal strain at the anterior cortical shell, where the major stress distribution was applied (Fig. 5). These findings strongly suggest that the anterior cortical bone shell is the strongest determinant of vertebral body compressive strength. This might have important implications in terms of the benefits of teriparatide treatment, as it appears that teriparatide builds bone predominantly in the most effective region to increase the entire strength of the skeleton (Fig. 5). This may be reflected in the finding that, compared with various other anti-osteoporotic agents tested to date, teriparatide has potent fracture prevention efficacy for the vertebral column [17,31].

As reported previously in a study using ovariectomized monkeys [32], vertebral cancellous bone volume was not decreased by ovariectomy despite an obvious decrease in all the mechanical properties in this study. Our results may imply that the increased fragility of vertebral bodies following ovariectomy is mainly derived from a decrease in cortical bone mass. Few previous studies have reported the effect of ovariectomy on the vertebral cortical shell in relation to mechanical strength in cynomolgus monkeys. One study showed that lumbar cortical thickness and compressive strength were not significantly changed following ovariectomy; however, how cortical thickness was evaluated was not precisely described [33]. Here, we evaluated cortical bone mass using multi-planar reconstruction of μCT imaging for a precise assessment, and found significant cortical bone loss following ovariectomy in both the sagittal and axial planes. In primates, the change in cortical bone in response to ovariectomy may be more sensitive than we

Table 3
Mechanical properties of L4 vertebrae.

	SHAM(n = 19)	OVX(n = 19)	LOW(n = 19)	HIGH(n = 20)
Maximum load (N)	2412.6 ± 360.2	2018.0 ± 467.9*	2195.4 ± 292.7	2205.5 ± 502.2
Stiffness (N/mm)	8962.3 ± 1328.6	7683.6 ± 1336.2*	8492.2 ± 1382.1	7749.6 ± 1558.7*
Energy absorption (mJ)	618.3 ± 146.9	473.1 ± 163.4*	545.9 ± 129.8	615.3 ± 214.3#
Ultimate stress (N/mm^2)	25.0 ± 4.64	21.5 ± 5.05*	24.1 ± 4.94	23.7 ± 5.72
Elastic modulus (MPa)	569.3 ± 119.8	508.5 ± 111.2	570.3 ± 121.0	518.8 ± 126.1
Toughness (MJ/m^3)	1.06 ± 0.32	0.81 ± 0.28*	0.99 ± 0.31	1.07 ± 0.37#

Values are expressed as mean ± SD.
* $P < 0.05$ vs. SHAM.
# $P < 0.05$ vs. OVX.

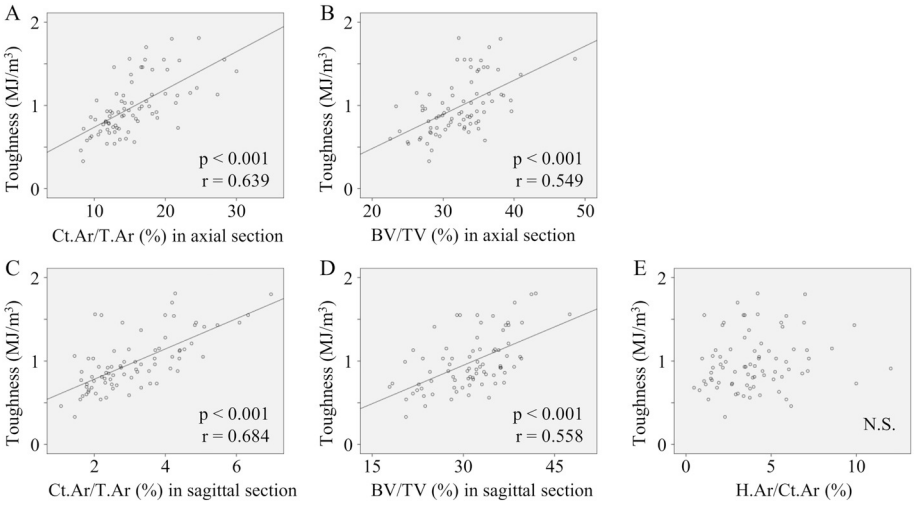

Fig. 4. Correlation between toughness and anterior cortical area fraction (Ct.Ar/T.Ar), cancellous bone volume (BV/TV), and cortical porosity (H·Ar/Ct.Ar) in all four groups. Pearson's product-moment correlation coefficient (r) was higher in the cortical area fraction (A, C) than in the cancellous bone volume (B, D) in each section obtained from mid-axial section of L3 (A,B) and mid-sagittal section of L7 (C, D). There was no significant correlation between toughness and cortical porosity (E).

previously thought. This indicates the importance of a thorough evaluation of the cortical shell in primates to clarify the mechanism of fragility fractures occurring in postmenopausal women.

The number of Haversian canals was decreased following ovariectomy in this study. This was unexpected, because increased intracortical bone remodeling by OVX would be expected to increase the number of Haversian canals. Although we cannot provide a plausible explanation for this phenomenon, the thinning of the anterior cortical shell due to OVX may restrict the number of Haversian canals that can form. Hence, the pronounced decrease in cortical bone mass might lead to a lack of intracortical remodeling space.

In the current study, teriparatide treatment did not increase bone formation parameters in either the periosteal and endocortical surfaces when compared with the OVX group even though bone mass of the anterior cortical shell was significantly increased. In the intracortical region, intracortical porosity, estimated by H.Ar/Ct.Ar, was not changed whereas H.MAR was increased following weekly teriparatide treatment. This is in contrast with the findings reported by Burr et al. [9], where endocortical MS/BS and intracortical porosity were significantly increased in the midshaft of the humerus in ovariectomized monkeys treated daily with teriparatide for 18 months. There are several explanations for these discrepancies. First, the dosage of teriparatide in our study was lower, which may have affected the rate of bone formation. Second, our treatment regimen was weekly rather than daily; in terms of bone turnover markers, it is likely that weekly teriparatide treatment stimulates less bone formation [17] than daily treatment [34], as shown in clinical studies. Finally, 18 months of a weekly treatment regimen might be too long to detect increased bone formation. Because the anterior cortical bone shell of the lumbar vertebra was thickened in our study, bone formation in the cortical surfaces may have been elevated or might have shown differences in the early phase of the experiment, and this may have reached a plateau by the end of our experiment at 18 months.

Table 5
Multiple regression analysis between toughness and structural parameters.

Multiple regression model	β		R^2
L3 mid-axial section	Ct.Ar/T.Ar (%)	0.598*	0.657
	BV/TV (%)	0.501*	
L7 mid-sagittal section	Ct.Ar/T.Ar (%)	0.557*	0.578
	BV/TV (%)	0.347*	

β: standardized partial regression coefficient.
R^2: coefficient of determination.
* $P < 0.001$; significant correlation between toughness and parameters.

One of the key differences between daily and weekly teriparatide treatment is the structural changes to the Haversian system in the cortical bone. A previous report showed that cortical porosity was increased by daily but not by weekly teriparatide treatment, even at the equivalent dose [35]. In fact, we found unremarkable changes in cortical porosity with weekly teriparatide treatment. By contrast, H.N was decreased by ovariectomy, and this decrease was inhibited by high-dose teriparatide treatment, suggesting that the structure of the Haversian canals was well preserved in the vertebral anterior cortical shell of monkeys treated with weekly teriparatide. Because the Haversian canals play an important role in intracortical remodeling [36,37], an intact structure of canals may preserve the vertebral cortical bone and maintain the surfaces available for intracortical remodeling. In previous work, the histological intracortical structure was evaluated only in terms of changes in cortical porosity on axial or transverse planes. In contrast, we analyzed Haversian structure in the sagittal plane of the anterior cortical shell using a parallel plate model [24]. Although the Haversian indices obtained from the plate model may require a validation study to compare these indices with the parameters obtained using direct methods (i.e., such as those performed in the early era of

Table 4
Correlation between structural and mechanical parameters.

	Maximum load (N)	Stiffness (N/mm)	Energy absorption (mJ)	Ultimate stress (N/mm^2)	Elastic modulus (MPa)	Toughness (MJ/m^3)
L3 Ct.Ar/T.Ar (%)	0.505***	0.448***	0.510***	0.678***	0.563***	0.639***
L3 BV/TV (%)	0.338**	0.255*	0.428***	0.541***	0.432***	0.549***
L7 Ct.Ar/T.Ar (%)	0.563***	0.406***	0.682***	0.594***	0.412***	0.684***
L7 BV/TV (%)	0.600***	0.516***	0.551***	0.579***	0.428***	0.558***
L7 H.Ar/Ct.Ar (%)	0.116	0.021	0.184	0.123	0.051	0.169

Values are expressed as Pearson's product-moment correlation coefficient.
* $P < 0.05$.
** $P < 0.01$.
*** $P < 0.001$.

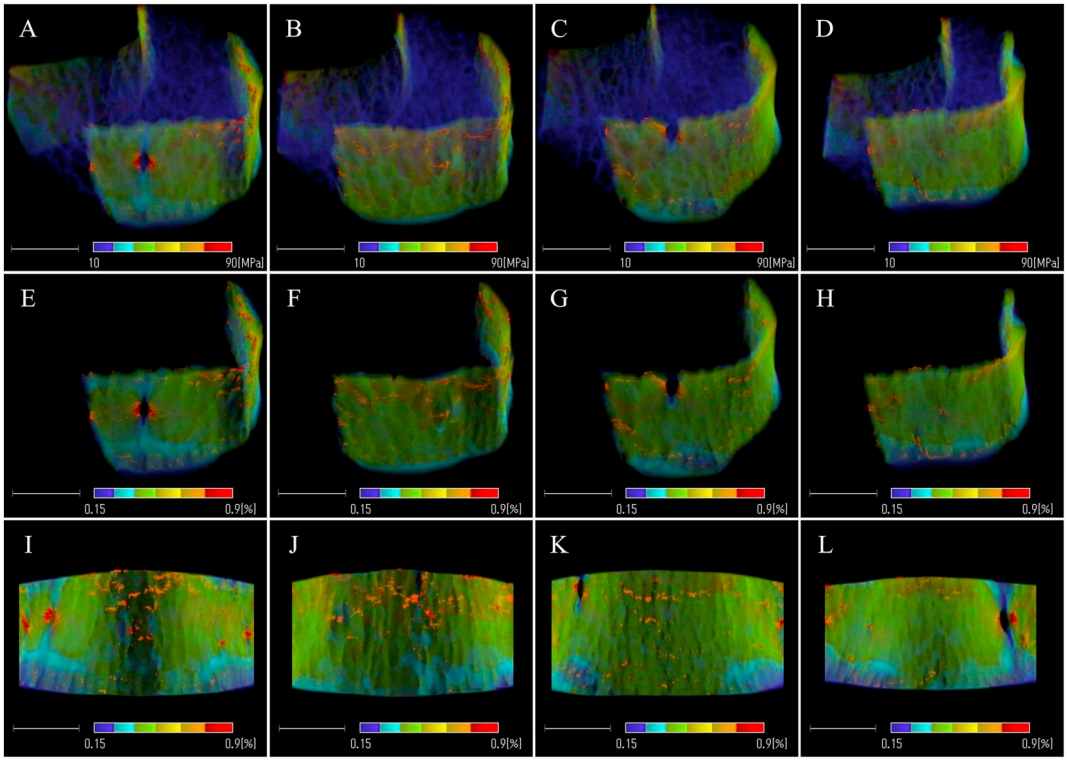

Fig. 5. Finite element analysis for the distribution of von Mises stress (A–D) and minimum principal strain from cranio-lateral (E–H) and anterior (I–L) views. Mean energy absorption is shown for SHAM (A, E, I), OVX (B, F, J), LOW (C, G, K), and HIGH (D, H, L) groups. Stress distribution was pronounced at the cortical shell in all groups (A–D). OVX group showed increased minimum principal strain at the anterior cortical shell when compared with the SHAM group. Minimum principal strain at the anterior cortical shell was decreased by teriparatide treatment in a dose-dependent fashion (E–L). Scale bars, 3 mm.

bone histomorphometry [23]), this stereological method is quite useful for quantifying the intracortical structure of Haversian canals in the longitudinal plane along the direction of the basic multicellular unit for intracortical remodeling [36,37]. Indeed, a stereological evaluation of the structure of the Haversian canal may facilitate a greater understanding of the changes to intracortical structures that are induced by teriparatide treatment.

Several limitations in this study should be acknowledged. First, dynamic histomorphometry was performed only in the sagittal section; therefore, the conventional intracortical histomorphometric measurements usually performed on transverse sections of long bones were not performed. Thus, data regarding the intracortical remodeling of the vertebral cortical shell in the current study may not be comparable with data from previous studies. Second, we were unable to histomorphometrically evaluate bone resorption. The differential effects on bone resorption between daily and weekly treatment protocols, as shown in clinical observations from bone markers, have not been clarified in histological examinations. Finally, caution is necessary when interpreting the data in terms of clinical relevance because the thickened anterior vertebral cortical shell was observed only in the HIGH teriparatide group, in which the monkeys received five times the clinical dose used in the treatment of osteoporosis in humans. Whether teriparatide at the clinical dose can increase the thickness of the vertebral cortical shell or improve the strength of the whole vertebral column in humans will be the subject of future study.

Through histomorphometric and biomechanical evaluations of the lumbar vertebra in ovariectomized cynomolgus monkeys treated with weekly teriparatide for 18 months, we conclude that: (1) bone mass of the anterior cortical shell and mechanical strength of the lumbar vertebral body were significantly increased by teriparatide treatment in a dose-dependent fashion; (2) the elevated mechanical properties of the whole lumbar vertebra were more associated with the increase in bone mass of the anterior cortical shell than with the increase in cancellous bone volume; and (3) the intracortical Haversian canal structure was preserved in the thickened anterior cortical shell generated in response to teriparatide treatment.

Conflict of interest statements

R Takao-Kawabata is an employee of Asahi Kasei Pharma Corporation.

Acknowledgments

This work was funded by Asahi Kasei Pharma Corporation. The authors wish to express their appreciation to Mr. N. Nango (RATOC System Engineering Corp., Tokyo, Japan) for technical support in finite element analysis, and to Ms. M. Higashihara and Ms. Y. Agawa for preparing undecalcified bone sections. We thank Edanz Group (www.edanzediting.com/ac) for editing a draft of this manuscript.

Authors' roles

Study design: RF, TM, and RTK. Study conduct: RF, TM, and RTK. Data collection: RF, SY, and RTK. Data analysis: RF and TM. Data interpretation: RF, SK, KI, and TM. Drafting manuscript: RF, TM, and TY.

References

[1] P.M. Camacho, S.M. Petak, N. Binkley, B.L. Clarke, S.T. Harris, D.L. Hurley, M. Kleerekoper, E.M. Lewiecki, P.D. Miller, H.S. Narula, R. Pessah-Pollack, V. Tangpricha, S.J. Wimalawansa, N.B. Watts, American association of clinical endocrinologists and american college of endocrinology clinical practice guidelines for the diagnosis and treatment of postmenopausal osteoporosis — 2016, Endocr. Pract. 22 (2016) 1–42, https://doi.org/10.4158/EP161435.GL.

[2] R.R. Recker, S.P. Bare, S.Y. Smith, A. Varela, M.A. Miller, S.A. Morris, J. Fox, Cancellous and cortical bone architecture and turnover at the iliac crest of postmenopausal osteoporotic women treated with parathyroid hormone 1-84, Bone 44

(2009) 113–119, https://doi.org/10.1016/j.bone.2008.09.019.
[3] Y. Jiang, J.J. Zhao, B.H. Mitlak, O. Wang, H.K. Genant, E.F. Eriksen, Recombinant human parathyroid hormone (1-34) [teriparatide] improves both cortical and cancellous bone structure, J. Bone Miner. Res. 18 (2003) 1932–1941, https://doi.org/10.1359/jbmr.2003.18.11.1932.
[4] M. Sato, M. Westmore, J. Clendenon, S. Smith, B. Hannum, G.Q. Zeng, R. Brommage, C.H. Turner, Three-dimensional modeling of the effects of parathyroid hormone on bone distribution in lumbar vertebrae of ovariectomized cynomolgus macaques, Osteoporos. Int. 11 (2000) 871–880, https://doi.org/10.1007/s001980070047.
[5] K.-Q. Zhang, J.-W. Chen, Q.-N. Li, G.-F. Li, X.-Y. Tian, L.-F. Huang, L.-H. Bao, M.-L. Wang, Effect of intermittent injection of recombinant human parathyroid hormone on bone histomorphometry of ovariectomized rats, Acta Pharmacol. Sin. 23 (2002) 659–662 http://www.ncbi.nlm.nih.gov/pubmed/12100763.
[6] J.E.M. Brouwers, B. Van Rietbergen, R. Huiskes, K. Ito, Effects of PTH treatment on tibial bone of ovariectomized rats assessed by in vivo micro-CT, Osteoporos. Int. 20 (2009) 1823–1835, https://doi.org/10.1007/s00198-009-0882-5.
[7] S. Sehmisch, M. Erren, T. Rack, M. Tezval, D. Seidlova-Wuttke, J. Richter, W. Wuttke, K.M. Stuermer, E.K. Stuermer, Short-term effects of parathyroid hormone on rat lumbar vertebrae, Spine (Phila Pa 1976) 34 (2009) 2014–2021, https://doi.org/10.1097/BRS.0b013e3181afe846.
[8] S.A. Gittens, G.R. Wohl, R.F. Zernicke, J.R. Matyas, P. Morley, H. Uludag, Systemic bone formation with weekly PTH administration in ovariectomized rats, J. Pharm. Pharm. Sci. 7 (2004) 27–37 http://www.ncbi.nlm.nih.gov/pubmed/15144732.
[9] D.B. Burr, T. Hirano, C.H. Turner, C. Hotchkiss, R. Brommage, J.M. Hock, Intermittently administered human parathyroid hormone(1-34) treatment increases intracortical bone turnover and porosity without reducing bone strength in the humerus of ovariectomized cynomolgus monkeys, J. Bone Miner. Res. 16 (2001) 157–165, https://doi.org/10.1359/jbmr.2001.16.1.157.
[10] M. Sato, M. Westmore, Y.L. Ma, A. Schmidt, Q.Q. Zeng, E.V. Glass, J. Vahle, R. Brommage, C.P. Jerome, C.H. Turner, Teriparatide [PTH(1-34)] strengthens the proximal femur of ovariectomized nonhuman primates despite increasing porosity, J. Bone Miner. Res. 19 (2004) 623–629, https://doi.org/10.1359/JBMR.040112.
[11] M. Ito, R. Oishi, M. Fukunaga, T. Sone, T. Sugimoto, M. Shiraki, Y. Nishizawa, T. Nakamura, The effects of once-weekly teriparatide on hip structure and biomechanical properties assessed by CT, Osteoporos. Int. 25 (2014) 1163–1172, https://doi.org/10.1007/s00198-013-2596-y.
[12] J. Borggrefe, C. Graeff, T.N. Nickelsen, F. Marin, C.C. Glüer, Quantitative computed tomographic assessment of the effects of 24 months of teriparatide treatment on 3D femoral neck bone distribution, geometry, and bone strength: results from the EUROFORS study, J. Bone Miner. Res. 25 (2010) 472–481, https://doi.org/10.1359/jbmr.090820.
[13] J.R. Zanchetta, C.E. Bogado, J.L. Ferretti, O. Wang, M.G. Wilson, M. Sato, G.A. Gaich, G.P. Dalsky, S.L. Myers, Effects of teriparatide [recombinant human parathyroid hormone (1-34)] on cortical bone in postmenopausal women with osteoporosis, J. Bone Miner. Res. 18 (2003) 539–543, https://doi.org/10.1359/jbmr.2003.18.3.539.
[14] A. Vesterby, L. Mosekilde, H.J.G. Gundersen, F. Melsen, L. Mosekilde, K. Holme, S. Sørensen, Biologically meaningful determinants of the in vitro strength of lumbar vertebrae, Bone 12 (1991) 219–224, https://doi.org/10.1016/8756-3282(91)90044-J.
[15] M.A. Haidekker, R. Andresen, H.J. Werner, Relationship between structural parameters, bone mineral density and fracture load in lumbar vertebrae, based on high-resolution computed tomography, quantitative computed tomography and compression tests, Osteoporos. Int. 9 (1999) 433–440, https://doi.org/10.1007/s001980050168.
[16] P. Chen, C.P. Jerome, D.B. Burr, C.H. Turner, Y.L. Ma, A. Rana, M. Sato, Interrelationships between bone microarchitecture and strength in ovariectomized monkeys treated with teriparatide, J. Bone Miner. Res. 22 (2007) 841–848, https://doi.org/10.1359/jbmr.070310.
[17] T. Nakamura, T. Sugimoto, T. Nakano, H. Kishimoto, M. Ito, M. Fukunaga, H. Hagino, T. Sone, H. Yoshikawa, Y. Nishizawa, T. Fujita, M. Shiraki, Randomized teriparatide [human parathyroid hormone (PTH) 1-34] once-weekly efficacy research (TOWER) trial for examining the reduction in new vertebral fractures in subjects with primary osteoporosis and high fracture risk, J. Clin. Endocrinol. Metab. 97 (2012) 3097–3106, https://doi.org/10.1210/jc.2011-3479.
[18] M. Saito, K. Marumo, Y. Kida, C. Ushiku, S. Kato, R. Takao-Kawabata, T. Kuroda, Changes in the contents of enzymatic immature, mature, and non-enzymatic senescent cross-links of collagen after once-weekly treatment with human parathyroid hormone (1–34) for 18 months contribute to improvement of bone strength in ovariectomized monkeys, Osteoporos. Int. 22 (2011) 2373–2383, https://doi.org/10.1007/s00198-010-1454-4.
[19] M.L. Bouxsein, S.K. Boyd, B.A. Christiansen, R.E. Guldberg, K.J. Jepsen, R. Müller, Guidelines for assessment of bone microstructure in rodents using micro-computed tomography, J. Bone Miner. Res. 25 (2010) 1468–1486, https://doi.org/10.1002/jbmr.141.
[20] W.S. Rasband, ImageJ, U. S. Natl. Institutes Heal. Bethesda, Maryland, USA, https://imagej.nih.gov/ij/, (2018) , Accessed date: 12 October 2018.
[21] X.Y. Tong, M. Malo, I.S. Tamminen, H. Isaksson, J.S. Jurvelin, H. Kröger, Development of new criteria for cortical bone histomorphometry in femoral neck: intra- and inter-observer reproducibility, J. Bone Miner. Metab. 33 (2015) 109–118, https://doi.org/10.1007/s00774-014-0562-1.
[22] W.A. Merz, R.K. Schenk, Quantitative structural analysis of human cancellous bone, Acta Anat. (Basel) 75 (1970) 54–66 http://www.ncbi.nlm.nih.gov/pubmed/5474733.
[23] W.J. Whitehouse, The quantitative morphology of anisotropic trabecular bone, J. Microsc. 101 (1974) 153–168, https://doi.org/10.1111/j.1365-2818.1974.tb03878.x.
[24] A.M. Parfitt, C.H. Mathews, A.R. Villanueva, M. Kleerekoper, B. Frame, D.S. Rao, Relationships between surface, volume, and thickness of iliac trabecular bone in aging and in osteoporosis. Implications for the microanatomic and cellular mechanisms of bone loss, J. Clin. Invest. 72 (1983) 1396–1409, https://doi.org/10.1172/JCI111096.
[25] D.W. Dempster, J.E. Compston, M.K. Drezner, F.H. Glorieux, J.A. Kanis, H. Malluche, P.J. Meunier, S.M. Ott, R.R. Recker, A.M. Parfitt, Standardized nomenclature, symbols, and units for bone histomorphometry: a 2012 update of the report of the ASBMR Histomorphometry nomenclature committee, J. Bone Miner. Res. 28 (2013) 2–17, https://doi.org/10.1002/jbmr.1805.
[26] D.R. Carter, W.C. Hayes, The compressive behavior of bone as a two-phase porous structure, J. Bone Joint Surg. Am. 59 (1977) 954–962 http://www.ncbi.nlm.nih.gov/pubmed/561786.
[27] R. Takao-Kawabata, Y. Isogai, A. Takakura, Y. Shimazu, E. Sugimoto, O. Nakazono, I. Ikegaki, H. Kuriyama, S. Tanaka, H. Oda, T. Ishizuya, Three-times-weekly administration of teriparatide improves vertebral and peripheral bone density, microarchitecture, and mechanical properties without accelerating bone resorption in ovariectomized rats, Calcif. Tissue Int. 97 (2015) 156–168, https://doi.org/10.1007/s00223-015-9998-0.
[28] S.K. Boyd, E. Szabo, P. Ammann, Increased bone strength is associated with improved bone microarchitecture in intact female rats treated with strontium ranelate: a finite element analysis study, Bone 48 (2011) 1109–1116, https://doi.org/10.1016/j.bone.2011.01.004.
[29] K. Imai, Analysis of vertebral bone strength, fracture pattern, and fracture location: a validation study using a computed tomography-based nonlinear finite element analysis, Aging Dis. 6 (2015) 180–187, https://doi.org/10.14336/AD.2014.0621.
[30] T. Hirano, D.B. Burr, C.H. Turner, M. Sato, R.L. Cain, J.M. Hock, Anabolic effects of human biosynthetic parathyroid hormone fragment (1-34), LY333334, on remodeling and mechanical properties of cortical bone in rabbits, J. Bone Miner. Res. 14 (1999) 536–545, https://doi.org/10.1359/jbmr.1999.14.4.536.
[31] S. Prevrhal, J.H. Krege, P. Chen, H. Genant, D.M. Black, Teriparatide vertebral fracture risk reduction determined by quantitative and qualitative radiographic assessment, Curr. Med. Res. Opin. 25 (2009) 921–928, https://doi.org/10.1185/03007990902790993.
[32] S.Y. Smith, J. Jolette, C.H. Turner, Skeletal health: primate model of postmenopausal osteoporosis, Am. J. Primatol. 71 (2009) 752–765, https://doi.org/10.1002/ajp.20715.
[33] M.S. Ominsky, S.K. Boyd, A. Varela, J. Jolette, M. Felx, N. Doyle, N. Mellal, S.Y. Smith, K. Locher, S. Buntich, I. Pyrah, R.W. Boyce, Romosozumab improves bone mass and strength while maintaining bone quality in ovariectomized cynomolgus monkeys, J. Bone Miner. Res. 32 (2017) 788–801, https://doi.org/10.1002/jbmr.3036.
[34] A. Miyauchi, T. Matsumoto, T. Sugimoto, M. Tsujimoto, M.R. Warner, T. Nakamura, Effects of teriparatide on bone mineral density and bone turnover markers in Japanese subjects with osteoporosis at high risk of fracture in a 24-month clinical study: 12-month, randomized, placebo-controlled, double-blind and 12-month open-label phases, Bone 47 (2010) 493–502, https://doi.org/10.1016/j.bone.2010.05.022.
[35] R. Zebaze, R. Takao-Kawabata, Y. Peng, A.G. Zadeh, K. Hirano, H. Yamane, A. Takakura, Y. Isogai, T. Ishizuya, E. Seeman, Increased cortical porosity is associated with daily, not weekly, administration of equivalent doses of teriparatide, Bone 99 (2017) 80–84, https://doi.org/10.1016/j.bone.2017.03.042.
[36] A.M. Parfitt, Osteonal and hemi-osteonal remodeling: the spatial and temporal framework for signal traffic in adult human bone, J. Cell. Biochem. 55 (1994) 273–286, https://doi.org/10.1002/jcb.240550303.
[37] N.E. Lassen, T.L. Andersen, G.G. Pløen, K. Søe, E.M. Hauge, S. Harving, G.E.T. Eschen, J.M. Delaisse, Coupling of bone resorption and formation in real time: new knowledge gained from human Haversian BMUs, J. Bone Miner. Res. 32 (2017) 1395–1405, https://doi.org/10.1002/jbmr.3091.